THE JOURNAL OF BIOLOGICAL CHEMISTRY VOL. 287, NO. 52, pp. 43599–43606, December 21, 2012

The Structure of Sec12 Implicates Potassium Ion Coordination in Sar1 Activation*

Received for publication, September 15, 2012, and in revised form, October 25, 2012 Published, JBC Papers in Press, October 29, 2012, DOI 10.1074/jbc.M112.420141

Conor McMahon[‡], Sean M. Studer[§], Chaevia Clendinen[‡], Geoffrey P. Dann[‡], Philip D. Jeffrey[‡], and Frederick M. Hughson[‡1]

From the [‡]Department of Molecular Biology, Princeton University, Princeton, New Jersey 08544 and the [§]Department of Chemical Physiology, Scripps Research Institute, La Jolla, California 92037

Background: Sec12 is a GEF responsible for the initiation of COPII vesicle budding.
Results: The 1.36 Å crystal structure of yeast Sec12 is presented, together with *in vitro* and *in vivo* analysis of structure-guided mutants.
Conclusion: A potassium-stabilized "K loop" plays an unprecedented and critical role in GEF activity.
Significance: All of the key proteins for COPII vesicle budding have now been structurally characterized.

Coat protein II (COPII)-coated vesicles transport proteins and lipids from the endoplasmic reticulum to the Golgi. Crucial for the initiation of COPII coat assembly is Sec12, a guanine nucleotide exchange factor responsible for activating the small G protein Sar1. Once activated, Sar1/GTP binds to endoplasmic reticulum membranes and recruits COPII coat components (Sec23/24 and Sec13/31). Here, we report the 1.36 Å resolution crystal structure of the catalytically active, 38-kDa cytoplasmic portion of *Saccharomyces cerevisiae* Sec12. Sec12 adopts a β propeller fold. Conserved residues cluster around a loop we term the "K loop," which extends from the N-terminal propeller blade. Structure-guided site-directed mutagenesis, in conjunction with *in vitro* and *in vivo* functional studies, reveals that this region of Sec12 is catalytically essential, presumably because it makes direct contact with Sar1. Strikingly, the crystal structure also reveals that a single potassium ion stabilizes the K loop; bound potassium is, moreover, essential for optimum guanine nucleotide exchange activity *in vitro*. Thus, our results reveal a novel role for a potassium-stabilized loop in catalyzing guanine nucleotide exchange.

The generation of COPII[2]-coated transport vesicles, required within the secretory pathway for endoplasmic reticulum (ER)-to-Golgi trafficking, provides a well characterized model system for investigating vesicle budding (1, 2). The assembly of COPII coat components onto the ER membrane is initiated by Sec12, a transmembrane guanine nucleotide exchange factor (GEF) (3, 4). Sec12 catalyzes the exchange of GDP for GTP on the small GTPase Sar1. Nucleotide exchange produces a conformational change in Sar1 that leads to the exposure of its amphipathic N-terminal α-helix and an increase in its affinity for membranes (5). Thus activated, Sar1 recruits Sec23/24 heterodimers, forming the inner layer of the COPII coat (6–9). Sar1 and Sec23/24 then recruit Sec13/31 heterotetramers, which polymerize to form the outer "cage" layer of the coat (7–11).

Insertion of the Sar1 N terminus into the ER membrane contributes to the membrane curvature required for COPII-coated vesicle budding and fission of vesicles from ER membranes, whereas Sec23/24 and Sec13/31 participate in shaping the vesicle through an intrinsic ability to deform membranes (12). In addition to initiating budding, Sec12 has also been proposed to stabilize the COPII coat during the budding process by renewing GTP on Sar1 at the boundary of the budding vesicle (13).

X-ray structures have been determined for all of these COPII vesicle budding machinery components except Sec12 (5, 14, 15). The 38-kDa cytosolic portion of Sec12, which is responsible for its GEF activity (13), was previously predicted to adopt a β propeller fold based on alignment of divergent homologs (16). Experimental validation and high resolution structural information have, however, been lacking. Furthermore, only one structure of a β propeller GEF, RCC1 (regulator of chromosome condensation 1), has previously been reported (17). We have now determined the high resolution crystal structure of the cytosolic portion of *Saccharomyces cerevisiae* Sec12, revealing the expected β propeller decorated by a novel surface loop critical for GEF function. This "K loop" binds a potassium ion, which in turn enhances GEF activity, providing what is, to our knowledge, the first example of a monovalent metal ion playing a role in GEF function. Asn-40, previously shown to be essential for Sec12 activity (13), sits at the base of the K loop, where it acts as an anchor to stabilize the loop and surrounding region through an elaborate network of hydrogen bonds.

EXPERIMENTAL PROCEDURES

Purification and Expression of Sec12 and Sar1—The cytoplasmic portion of Sec12 from *S. cerevisiae* (residues 1–354, previously termed Sec12ΔCp (13) but hereafter called simply Sec12), fused at its C terminus to a hexahistidine tag, was produced in *Escherichia coli* (Rosetta) using the expression plasmid pET21b (Novagen). Cells were grown in either Luria-Bertani

* This work was supported, in whole or in part, by National Institutes of Health Grant R01 GM071574 (to F. M. H.).
The atomic coordinates and structure factors (codes 4H5I and 4H5J) have been deposited in the Protein Data Bank (http://wwpdb.org/).
[1] To whom correspondence should be addressed: Dept. of Molecular Biology, Princeton University, Princeton, NJ 08544. Tel.: 609-258-4982; Fax: 609-258-6730; E-mail: hughson@princeton.edu.
[2] The abbreviations used are: COPII, coat protein II; ER, endoplasmic reticulum; GEF, guanine nucleotide exchange factor.

medium or, for production of selenomethionine-substituted protein, in M9 minimal medium supplemented with 40 mg/liter selenomethionine. Cells were pelleted and resuspended in lysis buffer (20 mM Tris, pH 7.6, 200–250 mM NaCl, 5 mM imidazole, 1 mM dithiothreitol (DTT)) before being lysed using an Emulsiflex-C5 homogenizer (Avestin). The lysate was supplemented with 2.5 mM phenylmethylsulfonyl fluoride and 1 μl/ml Protease Inhibitor Mixture (Sigma), clarified by centrifugation, and then fractionated using His60 Ni Superflow Resin (Clontech) or Ni^{2+}-charged IMAC Sepharose 6 Fast Flow Resin (GE Healthcare). Sec12 to be used for crystallization was further purified by ion exchange chromatography on a Source Q 10/10 column (GE Healthcare), where it eluted in the flow-through, and size exclusion chromatography (Superdex 200 10/300 GL, GE Healthcare). Sec12 to be used for biochemical experiments was further purified by size exclusion chromatography (Superdex 200 16/60 or Superdex 13/300). Although three Sec12 peaks were generally observed during size exclusion chromatography, only the peak corresponding to the monomer molecular weight was retained. Small aliquots of Sec12 in 20 mM Tris, pH 7.6, 1 mM DTT, 100 (or 200) mM NaCl were flash frozen in liquid N_2 and stored at −80 °C.

S. cerevisiae Sar1 was produced as a C-terminally hexahistidine-tagged fusion protein using the expression plasmid pET21b and purified by Ni^{2+} affinity and size exclusion chromatographies as described above. Purified Sar1p was frozen and stored at −80 °C in 20 mM Tris, pH 7.6, 200 mM NaCl, 1 mM DTT.

Crystallization and Structural Determination of Sec12—Crystals of selenomethionine-labeled Sec12 were grown by sitting drop vapor diffusion from a 1:1 (v/v) mixture of protein stock (3.8 mg/ml) containing 20 mM Tris, pH 7.6, 100 mM NaCl, 1 mM DTT and precipitant solution containing 91 mM Tris, pH 8.0, 181 mM potassium citrate, pH 8.3, 22% (w/v) PEG 3350. Crystals grew with cell dimensions of $a = b = 189.5$ Å, $c = 53.4$ Å in space group $P6_4$ containing two molecules per asymmetric unit. Multiwavelength anomalous diffraction data were collected at the selenium K edge at beamline X29 of the National Synchrotron Light Source at Brookhaven National Laboratory. Data were processed using the HKL suite (18) (Table 1). Ten selenium atoms were located using the program SHELXD (19), and phases were calculated using the program SHARP (20). The structure was built into the experimentally phased map using the program COOT (21) and refined with PHENIX (22) using non-crystallographic symmetry restraints.

During refinement, one metal-binding site per monomer was observed in the electron density maps and was provisionally identified as either Ca^{2+} or K^+ (which have similar x-ray scattering properties). K^+ was present at approximately physiological concentration in the crystallization conditions. In addition, the apparent occupancy of the metal site was unaffected by the addition of 10 mM calcium chloride or the chelating agent EGTA (30 mM) or EDTA (10 mM) to the precipitant solution. Soaking crystals in mother liquor plus the Ca^{2+} homolog Ho^{3+} (as 25 mM holmium(III) chloride hexahydrate) was similarly without effect. On the other hand, soaking crystals in mother liquor plus the K^+ homolog Rb^+ (as 50 or 200 mM rubidium chloride) caused an increase in the electron density consistent with substitution of the K loop K^+ with Rb^+. Together, these observations led us to assign the metal site as K^+ rather than Ca^{2+}. As described under "Results," other alternatives, such as Na^+ or Mg^{2+}, were inconsistent with the refined metal occupancy (~1.0 for K^+) and metal-ligand distances.

Subsequently, we found alternative selenomethionine Sec12 crystallization conditions by using 100 mM Tris, pH 8, 400 mM KCl, 22% (w/v) PEG 3350 as the precipitant solution. These crystals grew in a second, higher resolution, crystal form in space group P1 with $a = 53.4$ Å, $b = 53.5$ Å, $c = 62.0$ Å, $\alpha = 81.7°$, $\beta = 73.4°$, $\gamma = 87.58°$ and two molecules in the asymmetric unit (Table 1). Data were collected to 1.35 Å at National Synchrotron Light Source beamline X29. The structure was phased by molecular replacement, using the program PHASER (23) with the $P6_4$ crystal structure as a model and refined using PHENIX. As with the $P6_4$ crystal form, the scattering at the metal binding site and the ligand-metal distances were consistent with one bound K^+ per K loop in each Sec12 monomer.

Transient State Kinetics—The GEF activity of purified Sec12 proteins was measured by tryptophan fluorescence essentially as described (13). Briefly, reactions were performed in HKM buffer (20 mM HEPES, pH 7.0, 160 mM potassium acetate (KOAc), 3.5 mM magnesium chloride) containing liposomes, prepared as described previously (24), at a final concentration of 0.32 mM. GTP was added to a final concentration of 4 μM, and the reactions were performed with 0.4 μM Sar1 and Sec12 (at the noted concentrations) at 27 °C. Sec12 concentration was determined by UV absorbance following denaturation as described (25). We note that this method gives concentration measurements that are 2.4-fold higher than and presumably more accurate than those obtained using the Bradford assay calibrated to bovine serum albumin. We found that measurements of specific activity were about 10-fold higher than previously reported (13), possibly reflecting improvements in the purification protocol. For example, only those fractions whose elution from a size exclusion column was consistent with monomeric Sec12 were retained for use in crystallographic and biochemical experiments.

To measure the GEF activity displayed by a particular Sec12 construct, Sar1 activation experiments were conducted using a range of Sec12 concentrations. For each concentration, the apparent rate constant of Sar1 activation ($k_{activation}$) was determined using single-exponential fitting of the fluorescence time course. $k_{activation}$ values were then plotted as a function of Sec12 concentration. The rate increases linearly with concentration according to the equation $k_{activation} = k_{spontaneous} + k_{exchange}\cdot[Sec12]$, where $k_{spontaneous}$ and $k_{exchange}$, both estimated by least squares fitting, are the rate constant for spontaneous nucleotide exchange and the GEF activity for a given Sec12 construct, respectively (13).

To test the impact of different monovalent cations on exchange activity, GEF assays were performed in which the KOAc was replaced with either 150 mM KCl or 150 mM NaCl. The pH of the HEPES buffer was adjusted with either KOH or NaOH, as appropriate. We note that for reactions performed in KCl, a small amount (~2 mM) of Na^+ was also present, because Sec12 and Sar1 stocks both contained NaCl.

TABLE 1
Data collection, phasing, and refinement statistics

	$P6_4$ MAD[a]			
	Peak	Inflection	Remote	*P1*
Data collection				
Wavelength (Å)	0.9792	0.9794	0.9640	1.075
Resolution (Å)	100–2.8 (2.9–2.8)[b]	100–2.8 (2.9–2.8)	100–2.6 (2.69–2.60)	50–1.35 (1.37–1.35)
Unique reflections	27,210	27,520	34,159	132,685
Completeness (%)	99.5 (99.1)	99.9 (100.0)	99.9 (99.8)	93.6 (79.8)
Redundancy	6.0 (5.3)	8.2 (7.2)	8.3 (7.4)	3.8 (3.5)
R-sym	0.122 (0.423)	0.147 (0.621)	0.105 (0.426)	0.063 (0.610)
$\langle I/\sigma_I \rangle$	9.5 (2.7)	10.1 (2.3)	11.7 (3.4)	16.2 (2.2)
Phasing				
Figure of merit		0.46		
Refinement				
Resolution (Å)			50–2.60 (2.64–2.60)	50–1.36 (1.38–1.36)
Reflections $F \geq 0\ \sigma_F$ (free)			34,138 (1,726)	132,033 (6,617)
Completeness (%)			99.9 (99)	94.5 (82)
R-factor (%)			17.87 (21.8)	17.86 (25.3)
R-free (%)			21.64 (27.6)	19.71 (28.9)
No. of atoms				
Protein			5,261	5,249
Water			86	428
Potassium			6	4
RMSD[c] bond lengths (Å)			0.011	0.011
RMSD bond angles (degrees)			1.189	1.248
Wilson *B*-factor (Å^2)			28.6	12.8
Average *B*-factors (Å^2)				
All			34.2	15.0
Main chain			32.8	12.1
Side chain			35.8	16.8
Solvent/ligand			33.9	21.7
Ramachandran plot				
Favored (%)			97.0	98.2
Allowed (%)			2.8	1.8
Outliers (%)			0.2	0.0
PDB[d] code			4H5J	4H5I

[a] Multiwavelength anomalous diffraction.
[b] Values in parentheses are for the highest resolution shell.
[c] RMSD, root mean square deviation.
[d] Protein Data Bank.

Yeast Methods—To set the stage for plasmid shuffling experiments, an *S. cerevisiae* heterozygous deletion *SEC12*/Δ*sec12* strain (strain background BY4743, Thermo Fisher Scientific) was transformed with the *CEN-URA* plasmid pRS416-*SEC12*. pRS416-*SEC12* contains *SEC12*, together with 460 bp of upstream and 455 bp of downstream flanking DNA, inserted into the XhoI and HindIII sites of pRS416 (26). Transformants were sporulated and dissected to obtain haploid *sec12*Δ cells, whose chromosomal deletion was complemented by pRS416-*SEC12*. pRS415 *CEN-LEU* wild-type and mutant *SEC12* plasmids were constructed in the same manner and were transformed into the pRS416-*SEC12*-complemented haploid strains for plasmid shuffling. Individual transformants were streaked onto 5-fluoroorotic acid plates to select against pRS416-*SEC12*; the plates were then incubated at 22, 30, or 37 °C.

RESULTS

X-ray Structure of the Sec12 Cytoplasmic Domain—COPII coat assembly is initiated by Sec12, a single-pass transmembrane protein (3, 4). The ER luminal domain of Sec12 is highly variable in length and sequence and thus presumably lacks a conserved function, whereas the cytosolic domain is somewhat more conserved and functions as a Sar1 GEF (13, 27). To develop a detailed understanding of the initiation of COPII-coated vesicle budding, we determined the 1.36 Å resolution crystal structure of the cytosolic portion (residues 1–354) of *S. cerevisiae* Sec12 (Table 1; see "Experimental Procedures"). The structure confirms a previous proposal, based on sequence analysis (16), that Sec12 adopts a seven-bladed β propeller fold with a "1 + 3 velcro ring closure"; *i.e.* the seventh propeller blade comprises one β-strand from the N terminus in combination with three β-strands from the C terminus (28) (Fig. 1*A*).

One contiguous region of the Sec12 surface contains most of the highly conserved solvent-accessible residues (Fig. 1*B*). In the center of this region is an extended loop (the K loop) that projects upward from the first propeller blade. Despite the low overall sequence conservation among Sec12 proteins from distantly related species, the K loop is formed by a universally conserved sequence motif, GGGG*XXXX*GΦ*X*N (where Φ represents a hydrophobic amino acid; rarely, the fifth glycine is instead serine or the final asparagine is instead aspartate; Fig. 2*A*). This conserved sequence motif, corresponding to residues 29–40, connects the central two β-strands of the first propeller blade (16). In all four monomers (two distinct monomers per asymmetric unit in each of two different crystal forms), the K loop adopts the same conformation: a vertical loop, reminiscent of a roller coaster inversion, which surrounds and is evidently stabilized by a metal ion (Fig. 2*B*).

As discussed below, all available evidence suggests that the K loop metal is a K^+ ion, coordinated in an octahedral geometry by the oxygens of five protein groups and a water molecule (Fig. 2*B*). Four of the five protein ligands are provided by the K loop itself (*green* in Fig. 2*B*); these include the side chain oxygen of

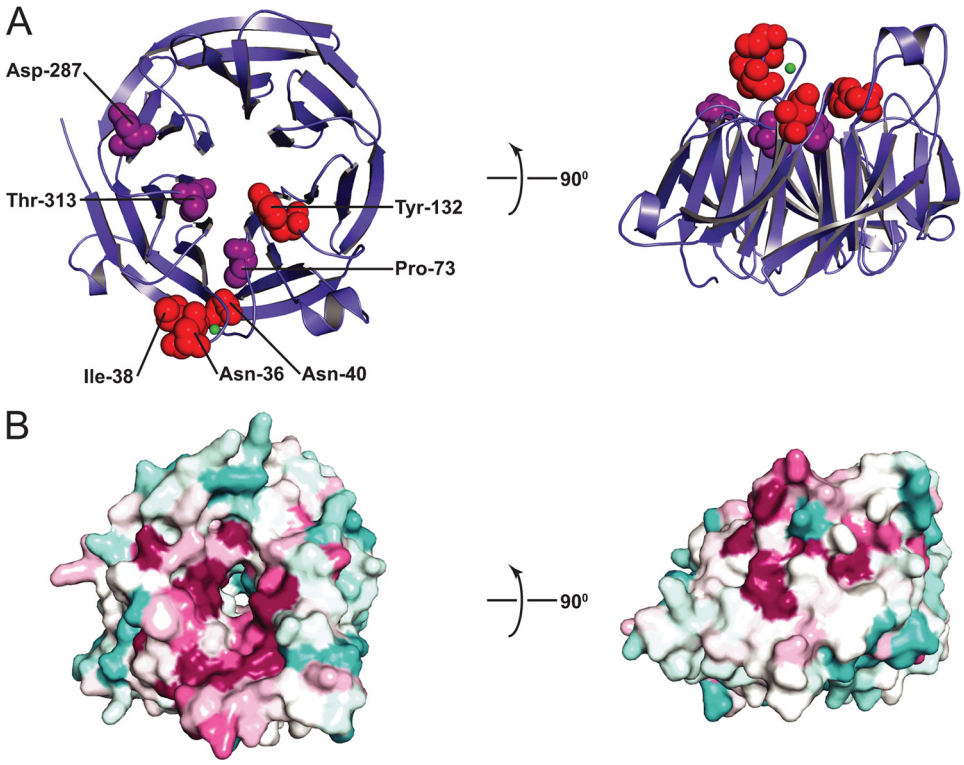

FIGURE 1. **X-ray structure of Sec12.** *A*, *ribbon representation* of the cytosolic domain of Sec12 (residues 1–354). Residues mutated in this work are shown in a *space-filling representation* and are *colored* to reflect the impact of the mutation on GEF activity *in vitro*, with *red* signifying <25% of wild-type specific exchange activity and *purple* signifying milder defects. The impact of N40A, P73L, and T313A mutations on GEF activity were described previously by Futai *et al.* (13). *B*, *surface representation* of the Sec12 structure, with sequence conservation represented in *colors* ranging from *burgundy* (most highly conserved) to *turquoise* (least highly conserved). These images were based on ConSurf analysis (36). The sequence alignment used to generate conservation scores contained primarily yeast Sec12 sequences, obtained by selecting only those sequences sharing at least 15% sequence identity with *S. cerevisiae* Sec12, residues 1–354.

A

```
S. cerevisiae     10 VGYPAYGAKFLNND-TLLVAGGGGEGNNGIPNKLTVLRVDPTK 51
K. lactis         12 IGYPVYGAKFLDNS-TLLVAGGGGEGNNGIPNKISALKVDFQK 53
P. pastoris        9 TGYPVYGAKFITKR-TLLTAGGGGEGNNGIPNKLSGFRIDFTK 50
D. melanogaster   15 VNFPLYAVDMLTSR-HILVAGGGGSSKTGVANGFEIYELYHNG 56
H. sapien         12 APFPLYALQVDPSTGLLIAAGGGGAAKTGIKNGVHFLQLELIN 54
C. albicans       11 VGYPIMGIKFLNNK-TILVAGGGGEGNNGIPNKITAIKSSFKV 52
P. falciparum      9 LNYPIYGIGSNKDY--VVTSGGGGGKNYGIEDMLDINIFNEKE 49
```

B

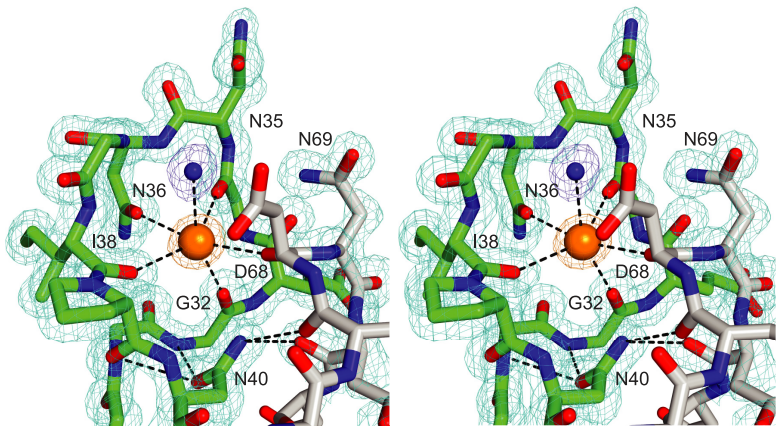

FIGURE 2. **The K loop region of Sec12.** *A*, sequence alignment. Much less homology is observed outside the K loop region of the cytoplasmic domain, and virtually no homology is observed in the luminal domain. *B*, *stereo view* of the K loop (*green*), adjacent loop (*gray*), and corresponding electron density ($2F_o - F_c$, contoured to 1σ). The bound K^+ and liganding water molecule are shown as a *large orange sphere* and a *small blue sphere*, respectively. The residues that contribute the remaining five oxygen ligands (except for Gly-34) are *labeled*. Also displayed is the hydrogen-bonding network centered on the functionally critical side chain of Asn-40.

Asn-36 and the backbone carbonyl oxygens of Gly-32, Gly-34, and Ile-38. The fifth protein ligand is the backbone carbonyl oxygen of Asp-68, a residue within a neighboring loop (residues 65–73; *gray* in Fig. 2*B*). The metal ion coordination is completed by a single water molecule. The relatively high *B*-factor for this water molecule hints that it could be displaced to allow

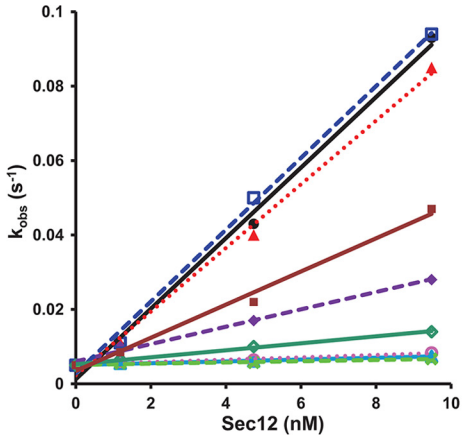

Sec12	$k_{exchange}$ (10^6 $s^{-1}M^{-1}$)	Relative exchange activity (%)
Wild-type	9.5 ± 0.6	100
N35A	8.6 ± 0.4	91
N36A	2.3 ± 0.2	24
I38D	0.24 ± 0.02	2.5
I38A	0.32 ± 0.05	3.3
N40A	0.16 ± 0.03	1.7
K41A	9.7 ± 0.4	102
Y132D	0.94 ± 0.04	9.9
D287K	4.5 ± 0.3	47

FIGURE 3. **Exchange activity of Sec12 mutants.** Tryptophan fluorescence nucleotide exchange assays measuring the GEF activity of Sec12 (wild type and single substitution mutants) were performed at various Sec12 concentrations. $k_{activation}$ values from each reaction (derived from exchange time courses, such as those shown in Fig. 4*A*) were plotted; the slope of these values, as determined by least squares fitting, is reported as the specific exchange activity ($k_{exchange}$; see "Experimental Procedures" for further details).

the bound K^+ to interact directly with Sar1. Thus, the water-filled ligand position on the K^+ ion might contribute directly to substrate binding, as observed for other enzymes (29) but not previously for nucleotide exchange factors.

Asn-40, previously proposed to act as a catalytic residue because of its strict conservation (16) and critical importance for GEF activity (13), instead plays a structural role, stabilizing both the K loop and the neighboring loop that provides the fifth protein ligand (Fig. 2*B*). Asn-40 fulfills this structural role by forming a network of hydrogen bonds with the backbone nitrogens of the strictly conserved residues Gly-31 and Gly-32 in the K loop and with the backbone carbonyls of Glu-67 and Asp-70 (flanking the liganding residue Asp-68) in the adjacent loop.

The Sec12 structure explains the strict conservation of the four glycines at the beginning of the K loop. Gly-32, whose carbonyl oxygen is one of the K^+ ligands, has a backbone conformation that lies in a region of the Ramachandran space excluded for non-glycine amino acids. The remaining glycines inhabit structural contexts where there is simply no room for a side chain larger than hydrogen. For example, any residue other than glycine at position 30 would collide with the absolutely conserved Asn-40, whereas any residue other than glycine at position 31 would collide with the conserved hydrophobic residue, Ile-38.

Conserved Surface Residues in and around the K Loop Are Critical for GEF Activity—To test the functional significance of the K loop (residues 29–40), we replaced several residues with Ala. We did not test substitutions for Gly (residues 29–32, 34, and 37) or Pro (residue 39) because of the concern that these would perturb the structure. Similarly, Glu-33, whose side chain forms two hydrogen bonds with Ser-91, was not altered. The four remaining K loop residues (Asn-35, Asn-36, Ile-38, and Asn-40), as well as the flanking residue Lys-41, were each replaced by Ala. To determine the activities of these mutants, we used an established *in vitro* GEF assay that relies on the change in Sar1 fluorescence upon replacement of GDP with GTP (13). As shown in Fig. 3, Ala substitution for Asn-36 (N36A), Ile-38 (I38A), and Asn-40 (N40A) reduced activity 75–98%; the other two substitutions had little or no impact on activity. Asn-36 is especially notable in that its side chain interacts directly with the bound metal (the other liganding groups are backbone carbonyls and a water molecule). Moreover, although Asn-36 is not one of the conserved residues within the K loop motif, multiple-sequence alignment indicates that this position is invariably occupied by a residue capable of interacting with a bound metal (*i.e.* either Asn, Ser, Thr, Tyr, or His). Nonetheless, although N36A retains only 25% of wild-type activity, it is not completely inactive. This finding may indicate that a bound metal is not absolutely required for activity; alternatively, it may indicate that a water molecule can take the place of the missing side chain ligand. Unfortunately, our inability to crystallize the N36A mutant prevented us from resolving this question definitively.

Ile-38 is strictly conserved as a hydrophobic residue (Φ) in the K loop. Its carbonyl oxygen interacts directly with the metal ion, whereas its side chain is surface exposed on the "back" side of the loop (as viewed in Fig. 2*B*). I38A retained only 3.3% of wild-type activity; a second mutant, I38D (substituting Ile-38 with Asp) was similarly inactive (2.6% of wild-type activity). Ile-38 thus appears to play a key role in GEF activity, perhaps interacting directly with Sar1. Finally, consistent with a previous report (13) and with the key structural role of Asn-40 as described above, we find that N40A has very little (<2%) residual activity.

In earlier work, several additional conserved residues proposed, based on the predicted β propeller structure, to lie on the top face of the propeller were investigated using site-directed mutagenesis (13). Two single substitutions, Pro-73 by Leu (P73L) and Thr-313 by Ala (T313A), displayed significantly (>50%) reduced GEF activity. However, although both residues map to the conserved regions of the x-ray structure (Fig. 1), both of their side chains are largely buried, and thus indirect structural effects cannot be excluded. We therefore tested the impact of changing the remaining conserved surface-exposed residues, Tyr-132 and Asp-287. There was a strong reduction in GEF activity, to 9.9% of wild type, when Tyr 132 was changed to aspartate (Y132D). Changing Asp-287, located on the outer edge of the conserved region, to Lys (D287K) had a milder impact (47% of wild-type activity).

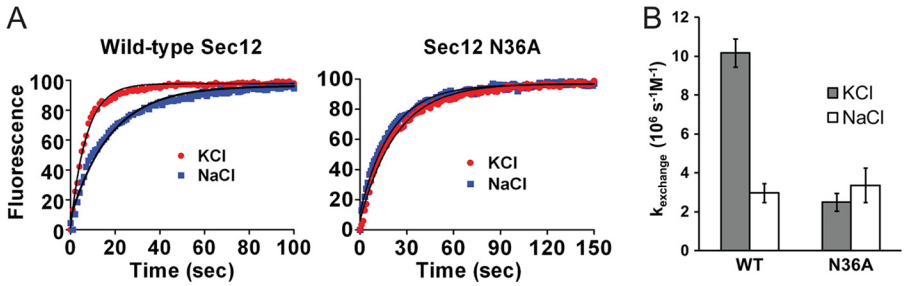

FIGURE 4. **K^+ enhances Sec12 GEF activity by binding to the K loop.** *A*, exchange assays with wild-type and N36A Sec12 were performed in the presence of Sec12 (9.5 nM). Conditions were as in Fig. 3 but with KCl or NaCl (each 150 mM) replacing potassium acetate. Fluorescence is shown in arbitrary units; representative time courses are shown together with fits to a single exponential. *B*, the corresponding $k_{exchange}$ values. *Error bars*, S.D. ($n = 3$).

The K Loop Binds Potassium, Enhancing GEF Activity—As described above, a single metal ion stabilizing the K loop was evident in electron density maps (Fig. 2). Multiple lines of evidence indicate that this metal ion is K^+. First, K^+ was present at near (180 mM) or above (400 mM) physiological concentrations in all of our successful crystallization experiments; no diffraction quality crystals could be grown in its absence. Second, the crystallographic occupancy for a single K^+ modeled in the K loop binding site refined to 0.98 and 0.86 for the two monomers within each asymmetric unit. This finding rules out the lighter elements Na^+ or Mg^{2+} but not the slightly heavier element Ca^{2+}. Third, the presence of the Ca^{2+} chelator EGTA or the multivalent cation chelator EDTA had no effect on crystallization or on the electron density observed at the metal position. Fourth, as predicted for a K^+ binding site, the electron density increased when Sec12 crystals were soaked in the K^+ analog Rb^+. Fifth, the observed metal-oxygen distances in our high resolution structure average 2.8 Å, which is much closer to the calculated optimum (assuming a six-ligand symmetrical coordination shell) for K^+ (2.77 Å) than Na^+ (2.46 Å) (29). Taken together, our results suggest strongly that the physiologically relevant K-loop-stabilizing metal ion is indeed K^+.

To determine whether K^+ modulates Sec12 function, GEF activity assays were performed in which the standard conditions were modified to exclude Na^+ or K^+, respectively. Consistent with an important role for K^+, the specific activity decreased 80% when K^+ was replaced with Na^+ (Fig. 4). To determine whether the stimulatory effect of K^+ is specifically attributable to K loop stabilization, we repeated the experiment using the N36A mutant. As described above, the K loop residue Asn-36 contains the only side chain that interacts directly with the bound K^+; the remaining ligands are contributed by main chain carbonyls and an ordered water molecule. Strikingly, the N36A mutant displayed the same specific activity in the presence and absence of K^+ (Fig. 4). These results support the conclusion that the binding of K^+ at physiological concentrations to the K loop results in a substantial increase in Sec12 GEF activity.

The K Loop Is Critical for Normal Growth of S. cerevisiae—To directly assess the physiological significance of the active site region of the Sec12 β propeller, we used plasmid shuffling to replace wild-type *SEC12*, which is essential for viability, with a battery of site-directed mutants. To ensure approximately wild-type expression levels, wild-type and mutant *SEC12* genes were carried on single-copy *CEN* plasmids together with ~500 nucleotides of flanking sequence on each side. We used single residue substitution mutants located within the K loop (Asn-35, Asn-36, Ile-38, or Asn-40) in the region surrounding the K loop (Tyr-15, Lys-41, Ser-72, or Tyr-132) or at the periphery of the conserved region (Glu-175 or Asp-287). The I38D and N40A mutations, which had the most severe effects of any mutants tested on GEF activity measured *in vitro* (Fig. 3), were lethal *in vivo* (Table 2). A second Ile-38 mutant, I38A, was not lethal but conferred a severe growth defect. These results demonstrate the essentiality of the K loop for *S. cerevisiae* viability. Our results also demonstrate that mutant Sec12 proteins retaining as little as 10% *in vitro* GEF activity were nonetheless capable of supporting apparently normal yeast growth, at least when expressed from a *CEN* plasmid in rich medium (compare Fig. 3 and Table 1). Thus, yeast containing the mutants N36A and Y132D, with 25 and 9.9% of wild-type GEF activity, respectively, as their sole source of Sec12 grew similarly to wild-type cells.

DISCUSSION

It has long been clear that GEF proteins have a wide variety of three-dimensional structures and use an array of mechanisms to destabilize the interaction between small GTPases and bound nucleotides (30). Our structure of Sec12 adds a second example of a β propeller GEF, similar in overall structure to the Ran GEF RCC1 (31). In both Sec12 and RCC1, small structural elements protruding from one propeller blade (a conserved, potassium-stabilized K loop in the case of Sec12, a "β wedge" in the case of RCC1 (17)) are crucial for GEF activity. A Ran-RCC1 co-crystal structure revealed that the β wedge pushes aside the P loop as a rigid body; a sulfate anion is found in the site normally occupied by the β phosphate of GDP/GTP and presumably serves to stabilize the conformation of the P loop in the absence of bound nucleotide (17). A Sar1-Sec12 co-crystal structure has proved elusive, presumably because of the very low affinity of Sec12 for Sar1 (13); similarly, given the large structural arrangements that GEFs generally provoke in GTPases (30), we have not attempted to dock the known Sar1 structure (5) with our Sec12 structure. Nonetheless, a working hypothesis is that the K loop interacts with the Sar1 P loop in a manner roughly analogous to that observed for the β wedge of RCC1 and Ran (Fig. 5). The rigidity of the β wedge of RCC1 appears to be important because its conformation remains essentially unchanged after binding to Ran (17, 31). K^+ may play a similar rigidifying role by stabilizing the K loop. In addi-

TABLE 2
Growth of wild-type and *sec12* mutant yeast

SEC12[a]	Growth[b]
Wild-type	+
pRS415[c]	−
N40A	−
I38D	−
I38A	+/−
Y15K	+
N35A	+
N36A	+
N36Q	+
K41A	+
S72A	+
Y132D	+
E175K	+
D287K	+

[a] Haploid *SEC12Δ S. cerevisiae* carrying pRS416-*SEC12* was transformed with pRS415-*SEC12* plasmids and then plated on 5-fluoroorotic acid to select against pRS416-*SEC12*.
[b] +, growth similar to wild-type; −, no growth (at 30 °C). I38A (+/−) displayed a significant growth defect at 30 °C, which was markedly exacerbated at 37 °C.
[c] pRS415 plasmid lacking SEC12.

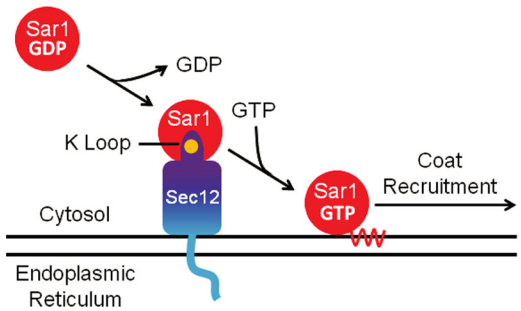

FIGURE 5. **Model of the interaction between Sec12 and Sar1.** One face of Sec12 is populated by conserved residues (*purple*), which interact with Sar1-GDP. The K loop helps to dislodge GDP from Sar1, perhaps by clashing with its P loop; this activity is enhanced by bound potassium (*orange*), which stabilizes the K loop. Following activation, Sar1 binds stably to the ER membrane and initiates COPII vesicle budding.

tion, the K^+ ion may participate directly in Sec12-Sar1/GDP binding. One attractive possibility is that the sixth K^+ ligand, a relatively weakly bound water molecule, is displaced in the Sec12-Sar1 complex by an oxygen ligand contributed by Sar1/GDP.

The catalytic importance of the K loop is clearly established by the strong impact, *in vitro* and *in vivo*, of mutations in conserved K loop residues. These include Ile-38, a surface-exposed K loop residue that probably interacts directly with Sar1, and Asn-40, which sits at the base of the K loop and stabilizes its conformation through an elaborate hydrogen bond network (Fig. 2*B*). Mutations in either residue cause catastrophic drops in catalytic activity *in vitro* (Fig. 3) and, as demonstrated by plasmid shuffling, are lethal *in vivo* (Table 2). The finding that all of the mutations that compromise function *in vivo* also display strongly reduced GEF activity *in vitro* is consistent with the expectation that GEF activity is, in fact, the physiologically essential function of Sec12.

Although the strict conservation of the GGGG*XXXX*GΦ*X*N motif that forms the K loop had been previously noted (16), its ability to coordinate K^+ was entirely unexpected. Two lines of evidence suggest that bound K^+ causes a marked increase in Sec12 GEF activity. First, mutation of Asn-36, whose side chain provides a liganding oxygen atom to the bound K^+, reduces *in vitro* GEF activity 4-fold. Second, substitution of K^+ by Na^+ in the *in vitro* assay reduces GEF activity about 5-fold. We note that each of these experiments might, in principle, underestimate the role of a bound metal. In the first case, it is possible that K^+ is still able to bind the N36A mutant, perhaps with water providing the missing ligand. In the second case, it remains possible that Na^+ can substitute, albeit imperfectly, for K^+. However, combining Na^+ substitution and N36A replacement did not diminish GEF activity further (Fig. 4). In any case, the level of rate enhancement observed in the presence of K^+ is in line with that observed for other enzymes activated by K^+ (or Na^+) (29).

Our work presents what is, to our knowledge, the first biochemical evidence supporting a role for a metal cation in stimulating GEF activity. Although several members of the RasGRP family of Ras GEFs contain potential Ca^{2+}-binding motifs (outside their catalytic domains) that have been implicated in Ca^{2+} regulation of GEF activity *in vivo* (32, 33), these conclusions remain controversial (34) and have not been validated *in vitro*. Mss4 was initially thought to function as a Zn^{2+}-stabilized GEF for the Rab protein Sec4, but its low GEF activity and the discovery that Sec2 is a much more efficient Sec4 GEF have led to its reclassification as a Rab chaperone (35). Thus, our results establish Sec12 as the first GEF whose catalytic domain is activated by metal ion binding.

Acknowledgments—We gratefully acknowledge the staff of National Synchrotron Light Source beamline X29 for assistance with data collection. We also thank Mark Rose and his group for helpful advice and reagents and especially Abigail Trarbach for assistance with yeast tetrad dissection.

REFERENCES

1. Lee, M. C., and Miller, E. A. (2007) Molecular mechanisms of COPII vesicle formation. *Semin. Cell Dev. Biol.* **18,** 424–434
2. Miller, E. A., and Barlowe, C. (2010) Regulation of coat assembly. Sorting things out at the ER. *Curr. Opin. Cell Biol.* **22,** 447–453
3. Barlowe, C., and Schekman, R. (1993) SEC12 encodes a guanine-nucleotide-exchange factor essential for transport vesicle budding from the ER. *Nature* **365,** 347–349
4. Nakano, A., Brada, D., and Schekman, R. (1988) A membrane glycoprotein, Sec12p, required for protein transport from the endoplasmic reticulum to the Golgi apparatus in yeast. *J. Cell Biol.* **107,** 851–863
5. Huang, M., Weissman, J. T., Beraud-Dufour, S., Luan, P., Wang, C., Chen, W., Aridor, M., Wilson, I. A., and Balch, W. E. (2001) Crystal structure of Sar1-GDP at 1.7 Å resolution and the role of the NH_2 terminus in ER export. *J. Cell Biol.* **155,** 937–948
6. Aridor, M., Weissman, J., Bannykh, S., Nuoffer, C., and Balch, W. E. (1998) Cargo selection by the COPII budding machinery during export from the ER. *J. Cell Biol.* **141,** 61–70
7. Matsuoka, K., Orci, L., Amherdt, M., Bednarek, S. Y., Hamamoto, S., Schekman, R., and Yeung, T. (1998) COPII-coated vesicle formation reconstituted with purified coat proteins and chemically defined liposomes. *Cell* **93,** 263–275
8. Matsuoka, K., Schekman, R., Orci, L., and Heuser, J. E. (2001) Surface structure of the COPII-coated vesicle. *Proc. Natl. Acad. Sci. U.S.A.* **98,** 13705–13709
9. Stagg, S. M., LaPointe, P., Razvi, A., Gürkan, C., Potter, C. S., Carragher, B., and Balch, W. E. (2008) Structural basis for cargo regulation of COPII coat assembly. *Cell* **134,** 474–484
10. Bi, X., Mancias, J. D., and Goldberg, J. (2007) Insights into COPII coat nucleation from the structure of Sec23.Sar1 complexed with the active fragment of Sec31. *Dev. Cell* **13,** 635–645

11. Shaywitz, D. A., Espenshade, P. J., Gimeno, R. E., and Kaiser, C. A. (1997) COPII subunit interactions in the assembly of the vesicle coat. *J. Biol. Chem.* **272,** 25413–25416
12. Lee, M. C., Orci, L., Hamamoto, S., Futai, E., Ravazzola, M., and Schekman, R. (2005) Sar1p N-terminal helix initiates membrane curvature and completes the fission of a COPII vesicle. *Cell* **122,** 605–617
13. Futai, E., Hamamoto, S., Orci, L., and Schekman, R. (2004) GTP/GDP exchange by Sec12p enables COPII vesicle bud formation on synthetic liposomes. *EMBO J.* **23,** 4146–4155
14. Bi, X., Corpina, R. A., and Goldberg, J. (2002) Structure of the Sec23/24-Sar1 pre-budding complex of the COPII vesicle coat. *Nature* **419,** 271–277
15. Fath, S., Mancias, J. D., Bi, X., and Goldberg, J. (2007) Structure and organization of coat proteins in the COPII cage. *Cell* **129,** 1325–1336
16. Chardin, P., and Callebaut, I. (2002) The yeast Sar exchange factor Sec12, and its higher organism orthologs, fold as β-propellers. *FEBS Lett.* **525,** 171–173
17. Renault, L., Kuhlmann, J., Henkel, A., and Wittinghofer, A. (2001) Structural basis for guanine nucleotide exchange on Ran by the regulator of chromosome condensation (RCC1). *Cell* **105,** 245–255
18. Otwinowski, Z., and Minor, W. (1998) Processing of x-ray diffraction data collected in oscillation mode. *Methods Enzymol.* **276,** 307–326
19. Sheldrick, G. M. (2008) A short history of SHELX. *Acta Crystallogr. A* **64,** 112–122
20. Bricogne, G., Vonrhein, C., Flensburg, C., Schiltz, M., and Paciorek, W. (2003) Generation, representation and flow of phase information in structure determination. Recent developments in and around SHARP 2.0. *Acta Crystallogr. D* **59,** 2023–2030
21. Emsley, P., Lohkamp, B., Scott, W. G., and Cowtan, K. (2010) Features and development of Coot. *Acta Crystallogr. D* **66,** 486–501
22. Adams, P. D., Grosse-Kunstleve, R. W., Hung, L. W., Ioerger, T. R., McCoy, A. J., Moriarty, N. W., Read, R. J., Sacchettini, J. C., Sauter, N. K., and Terwilliger, T. C. (2002) PHENIX. Building new software for automated crystallographic structure determination. *Acta Crystallogr. D* **58,** 1948–1954
23. Storoni, L. C., McCoy, A. J., and Read, R. J. (2004) Likelihood-enhanced fast rotation functions. *Acta Crystallogr. D* **60,** 432–438
24. Antonny, B., Madden, D., Hamamoto, S., Orci, L., and Schekman, R. (2001) Dynamics of the COPII coat with GTP and stable analogues. *Nat. Cell Biol.* **3,** 531–537
25. Edelhoch, H. (1967) Spectroscopic determination of tryptophan and tyrosine in proteins. *Biochemistry* **6,** 1948–1954
26. Sikorski, R. S., and Hieter, P. (1989) A system of shuttle vectors and yeast host strains designed for efficient manipulation of DNA in *Saccharomyces cerevisiae*. *Genetics* **122,** 19–27
27. Weissman, J. T., Plutner, H., and Balch, W. E. (2001) The mammalian guanine nucleotide exchange factor mSec12 is essential for activation of the Sar1 GTPase directing endoplasmic reticulum export. *Traffic* **2,** 465–475
28. Fülöp, V., and Jones, D. T. (1999) β propellers. Structural rigidity and functional diversity. *Curr. Opin. Struct. Biol.* **9,** 715–721
29. Page, M. J., and Di Cera, E. (2006) Role of Na^+ and K^+ in enzyme function. *Physiol. Rev.* **86,** 1049–1092
30. Bos, J. L., Rehmann, H., and Wittinghofer, A. (2007) GEFs and GAPs. Critical elements in the control of small G proteins. *Cell* **129,** 865–877
31. Renault, L., Nassar, N., Vetter, I., Becker, J., Klebe, C., Roth, M., and Wittinghofer, A. (1998) The 1.7 Å crystal structure of the regulator of chromosome condensation (RCC1) reveals a seven-bladed propeller. *Nature* **392,** 97–101
32. Ebinu, J. O., Bottorff, D. A., Chan, E. Y., Stang, S. L., Dunn, R. J., and Stone, J. C. (1998) RasGRP, a Ras guanyl nucleotide-releasing protein with calcium- and diacylglycerol-binding motifs. *Science* **280,** 1082–1086
33. Kawasaki, H., Springett, G. M., Toki, S., Canales, J. J., Harlan, P., Blumenstiel, J. P., Chen, E. J., Bany, I. A., Mochizuki, N., Ashbacher, A., Matsuda, M., Housman, D. E., and Graybiel, A. M. (1998) A Rap guanine nucleotide exchange factor enriched highly in the basal ganglia. *Proc. Natl. Acad. Sci. U.S.A.* **95,** 13278–13283
34. Stone, J. C. (2011) Regulation and function of the RasGRP family of Ras activators in blood cells. *Genes Cancer* **2,** 320–334
35. Itzen, A., Rak, A., and Goody, R. S. (2007) Sec2 is a highly efficient exchange factor for the Rab protein Sec4. *J. Mol. Biol.* **365,** 1359–1367
36. Ashkenazy, H., Erez, E., Martz, E., Pupko, T., and Ben-Tal, N. (2010) ConSurf 2010. Calculating evolutionary conservation in sequence and structure of proteins and nucleic acids. *Nucleic Acids Res.* **38,** W529–W533